Journal of Power Sources 196 (2011) 4342–4346

Contents lists available at ScienceDirect

Journal of Power Sources

journal homepage: www.elsevier.com/locate/jpowsour

Short communication

Deuteration properties of $CaNi_{5-x}Cu_x$ system

M. Retuerto[a,*], J. Sánchez-Benítez[a], J.A. Alonso[a], F. Leardini[b], J.R. Ares[b], J.F. Fernández[b], C. Sánchez[b]

[a] Instituto de Ciencia de Materiales de Madrid, C.S.I.C., Cantoblanco, E-28049 Madrid, Spain
[b] Laboratorio MIRE, Dpto. Física de Materiales, M04-206, UAM, Cantoblanco, E-28049 Madrid, Spain

ARTICLE INFO

Article history:
Received 12 January 2011
Accepted 16 January 2011
Available online 26 January 2011

Keywords:
Hydrogen storage
Metal hydrides
Neutron diffraction
$CaNi_5$

ABSTRACT

Intermetallic compounds with nominal formula $CaNi_{5-x}Cu_x$ ($x = 0, 1, 2.5$) have been prepared in order to investigate their hydrogenation properties. The samples were obtained by arc-melting and were deuterated in a Sieverts reactor. For $x = 0$ and 1, we have found that the fast kinetics and the different shape of the curve (non sigmoidal) in the second absorption process indicate an improvement of the hydrogen absorption due to the activation of the alloys. The deuterium desorption spectra are similar for $x = 0$ and 1 whereas for $x = 2.5$ the desorption ranges a broader temperature interval (~100–350 °C) indicating a certain degree of chemical inhomogeneity or amorphization intrinsic to the parent sample or induced by the deuterium absorption. The formed deuterides were passivated in the presence of air in order to carry out a neutron diffraction study, allowing us to determine the deuterium positions in the samples. While in $CaNi_4CuD_y$ the deuterium is randomly distributed over seven different positions, in $CaNi_5D_y$ the deuterium only occupies five of them. This wider distribution in $CaNi_4CuD_y$ can explain its higher stability, and therefore, its higher desorption temperature for deuterium.

1. Introduction

Nowadays, due to the increasing energy demand and issues related with environmental contamination, the development of new clean fuels and energy sources is becoming an active field of research. Hydrogen is a good candidate as energy vector because of its abundance and environmental affability. Many efforts have been directed to develop the hydrogen storage technology, since it was found that there are solid intermetallic materials that absorb hydrogen at higher volume densities than that for gas or liquid hydrogen [1,2]. The AB_5 family of intermetallic compounds is one of the most popular families of hydrogen storage compounds, mainly used as hydride electrode materials in Ni-MH batteries [3–6].

The best-known AB_5 hydrogen storage compound is $LaNi_5$, which forms a hydride with a maximum composition of $LaNi_5H_7$. Many substitutions have been carried out in $LaNi_5$ in order to optimise its hydrogenation properties: La has been replaced by Ce, Pr, Nd, Ca or Mischmetal (Mm) [7–9]; and Ni by Mn, Zn, Cr, Fe, Co, Cu or even Al and Sn [10–13].

The replacement of La by Ca is very attractive due to its lower cost and higher storage capacity (1.9 wt.%) [14,15], since the hydride can also achieve the composition $CaNi_5H_7$. However, the $CaNi_5H_x$ system is more complex since it presents a phase diagram with three plateaus [16] and it tends to disproportionate in $CaH_2 + 5Ni$ when it is hydrided, therefore it has an appalling cycling stability.

In this work we have tried to reduce the disproportionation problem replacing Ni by Cu in the family of intermetallic compounds $CaNi_{5-x}Cu_x$ ($x = 0, 1, 2.5$), in the search of new light materials for hydrogen storage. If a doped derivative of the cheap and light $CaNi_5$ intermetallic is found to have a long term stability in the hydride phase, avoiding the mentioned disproportionation, it will constitute an ideal material for hydrogen storage. Our work gives some steps in this direction. We have deuterated the samples in a Sieverts reactor and carried out a neutron powder diffraction (NPD) study on them, trying to determine the structural peculiarities of the new phases. We have used deuterium because it is easier to analyze than hydrogen by NPD since hydrogen presents an incoherent scattering that interferes in the diffraction pattern. With respect to the absorption process, in principle the maximum storage capacity should not change between hydrogen and deuterium, the same phase should be formed in both cases. However, the thermodynamic properties could be slightly affected (small differences in the plateau pressure) due to the isotopic effect: the use of deuterides instead of hydrides produces a decrease of the enthalpy of the compound (shift of the energetic levels) leading to a higher stability of the material (since the entropy moves in an opposite direction) [17]. So, we will also expect an effect in the kinetic of the reac-

* Corresponding author at: Instituto de Ciencia de Materiales de Madrid, Síntesis y Estructura de óxidos, Sor Juana Ines de la Cruz, 3, 28049 Madrid, Spain.
Tel.: +34 913349000; fax: +34 913720623.
E-mail address: mretuerto@icmm.csic.es (M. Retuerto).

0378-7753/$ – see front matter © 2011 Elsevier B.V. All rights reserved.
doi:10.1016/j.jpowsour.2011.01.071

tion, because the shift of the energy levels carries an increase of the activation energy of the reaction. Also, some changes in the absorption/desorption processes could be expected due to the different diffusion coefficients of hydrogen and deuterium. Nevertheless, most of the times these variations are not significant.

We have also performed thermal desorption spectroscopy in order to follow the deuterium desorption processes. It has been observed that there is a non-monotonic behaviour, and there is a loss of capacity from $x = 0$ to $x = 1$, finding a better capacity value for $x = 2.5$, although the desorption process expands into a wider and higher range of temperatures.

2. Experimental

$CaNi_{5-x}Cu_x$ ($x = 0$, 1.0, 2.5) alloys were prepared in an arc-melting furnace under an inert argon atmosphere (0.05 MPa, 99.999% vol. purity). The starting materials Ca, Ni and Cu, mixed in the nominal stoichiometry to form the alloys $CaNi_5$, $CaNi_4Cu$ and $CaNi_{2.5}Cu_{2.5}$, were melted into the furnace and then quenched in a water-cooled copper crucible. The melting process was repeated several times in order to assure the homogeneity of the samples.

The alloys were obtained as polycrystalline ingots. A small portion of the ingots was powdered to assess their purity and structure by X-ray diffraction (XRD) experiments. The deuteration of the alloys (weighted ~1 g) was performed in a Sieverts type reactor at room temperature and in a deuterium pressure range of 17–33 bar. Dynamic vacuum was used during the desorption processes. Once the absorption process has been repeated several times it was introduced air into the reactor chamber in order to passivate the surface of the deuterides, trying to avoid the deuterium desorption. Finally, the deuterated samples were kept in an argon atmosphere using a globe-box.

Thermal desorption spectroscopy (TDS) experiments have been performed by means of a differential scanning calorimeter (Perkin Elmer DSC-4) connected to a quadrupole mass spectrometer (QMS, Balzers, Mod. Prisma). Further details of the experimental setup are given elsewhere [17,18]. The experiments have been done on the deuterated samples to determine the quantity of absorbed deuterium and the kinetics of the deuterium desorption processes.

In a parallel way, neutron powder diffraction (NPD) data were collected on the high-resolution powder diffractometer D1A ($\lambda = 1.910$ Å) at room temperature at the ILL, Grenoble, France. The refinement of the crystal structures was performed by the Rietveld method [19], using the FULLPROF refinement program [20]. A pseudo-Voigt function was chosen to fit the diffraction peak shapes. The following parameters were refined in the final run of the D1A high-resolution data set: scale factor, background coefficients, zero-point error, pseudo-Voigt peak shape function corrected for asymmetry, positional coordinates and overall thermal factor.

3. Results and discussion

Fig. 1 shows the XRD diagrams of the compounds taken before and after the deuteration. For samples with $x = 0$ and 1 the XRD diagrams look very similar, except for the appearance of new peaks in the deuterated samples corresponding to $Ca(OD)_2$, probably formed due to the air exposure of the samples during the XRD measurements. The rest of the reflections can be indexed in the structural group of $CaCu_5$, which presents a hexagonal structure with space group *P*6/*mmm*. There is a small amount of Ni metal present in the samples. In the case of $CaNi_{2.5}Cu_{2.5}$, both the alloy and the deuterated sample have a crystal structure closer to $CaNi_3$ than to $CaNi_5$. Moreover, $CaNi_{2.5}Cu_{2.5}$ was not crystalline enough to perform NPD experiments. However, we have analysed the deuterium absorption and desorption on this sample by TDS.

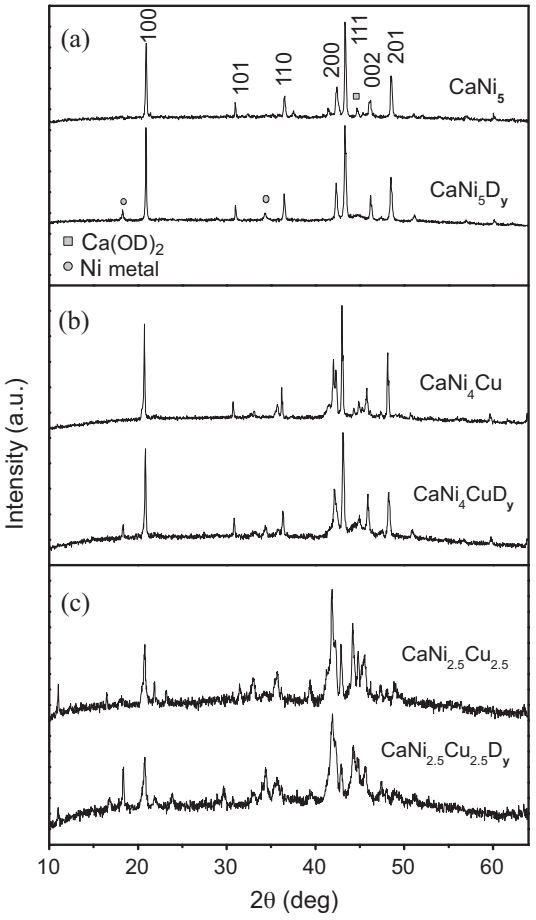

Fig. 1. X-ray powder diffraction patterns for (a) $CaNi_5$ and $CaNi_5D_y$, (b) $CaNi_4Cu$ and $CaNi_4CuD_y$, and (c) $CaNi_{2.5}Cu_{2.5}$ and $CaNi_{2.5}Cu_{2.5}D_y$, collected at room temperature with CuK_α radiation.

3.1. Deuteration

The deuteration of the alloys was carried out as follows: for $x = 0$ and 1 two deuteration cycles were performed and for sample with $x = 2.5$ only one absorption cycle was completed. Fig. 2a and b shows the first and second absorption curves for $CaNi_{5-x}Cu_x$ series, respectively. For $x = 0$ and $x = 1$, the shape of the curve for the second absorption cycle is different to the first one, since it does not follow a sigmoidal shape. Moreover, the kinetics is faster, since in the second cycle the deuterium is absorbed in a shorter time, indicating the improvement of the absorption process due to the activation of the alloys.

As it is observed in Fig. 2, the temperature of the sample increases during the deuteration because the absorption reaction is an exothermic process. During the second cycle, the temperature reached for the sample is higher than in the first cycle, due to the higher deuteration speed, not allowing the system to dissipate the heat.

The amount of deuterium absorbed by $CaNi_5$ in the first cycle is 7.15 D/f.u., while in the second process it is reduced to 6.3 D/f.u. In $CaNi_4Cu$, the sample is able to absorb 5.8 D/f.u. during the first cycle and 4.2 D/f.u. in the second one. In $CaNi_{2.5}Cu_{2.5}$ we have only performed one absorption cycle, in which the compound was able to absorb 6.8 D/f.u. Therefore, the quantity of deuterium absorbed by the $x = 2.5$ intermetallic compound is higher than that of the $x = 1$ alloy. The reason could be (i) the low crystallinity of $CaNi_{2.5}Cu_{2.5}$ sample, where the smaller size of the particles favours the absorption process, or (ii) the actual stoichiometry of this sample is similar

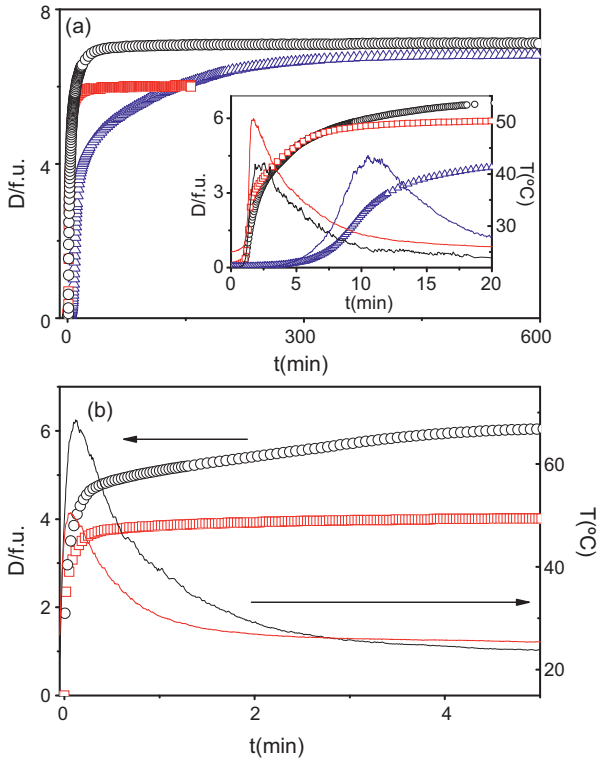

Fig. 2. (a) First and (b) second deuterium absorption cycles for $CaNi_5$ (black circles), $CaNi_4Cu$ (red squares) and $CaNi_{2.5}Cu_{2.5}$ (blue triangles) (P_{D2} = 17–33 bar). Inset of (a) shows a zoom of the initial minutes of the first absorption processes of all the compounds. The right axis and continuous lines in the figures represent the change of the temperature with the deuterium absorption. (For interpretation of the references to color in this figure legend, the reader is referred to the web version of the article)

to $CaNi_3$, being the storage capacity of $CaNi_3$ (~2.1 wt.%) higher than the capacity of $CaNi_5$ [21]. However, the kinetics of the process is slower than in samples with $x = 0$ and 1.

3.2. Thermal desorption spectroscopy experiments

We have carried out thermal desorption spectroscopy (TDS) experiments to analyze the deuterium contents of the deuterides immediately after the absorption process and also some hours later. TDS measurements allow us to obtain the deuterium desorption temperature. Fig. 3a and b illustrates the thermal desorption spectra of the $CaNi_5D_y$ deuteride, 24 h and 194 h after the absorption, respectively. Fig. 3a shows only one desorption peak associated with the desorption of $CaNi_5D_y$. However, Fig. 3b shows a different desorption behaviour: at 100–115 °C temperature range, a superposition of three different peaks appears, which corresponds to the desorption of $CaNi_5D_y$ and some inhomogeneties formed due to the disproportionation of the sample during the absorption–desorption processes. The desorption peak observed at ~375 °C, could be related to the desorption of CaD_2, segregated during the absorption process, since these deuterides are not stable and spontaneously decompose with time. This peak is also observed in Fig. 3a, but with much lower intensity.

Fig. 4 shows the thermal desorption spectra for the $CaNi_{5-x}Cu_xD_y$ series (Fig. 4a for $x = 0$, Fig. 4b for $x = 1$ and Fig. 4c for $x = 2.5$). As it can be observed in the figure, the desorption temperature of $CaNi_5D_y$ is 94 °C. In the case of $CaNi_4CuD_y$, the desorption temperature increases up to 100 °C, and in $CaNi_{2.5}Cu_{2.5}D_y$ the desorption occurs in a broad temperature range between 120 °C and 150 °C. This different behaviour could be ascribed

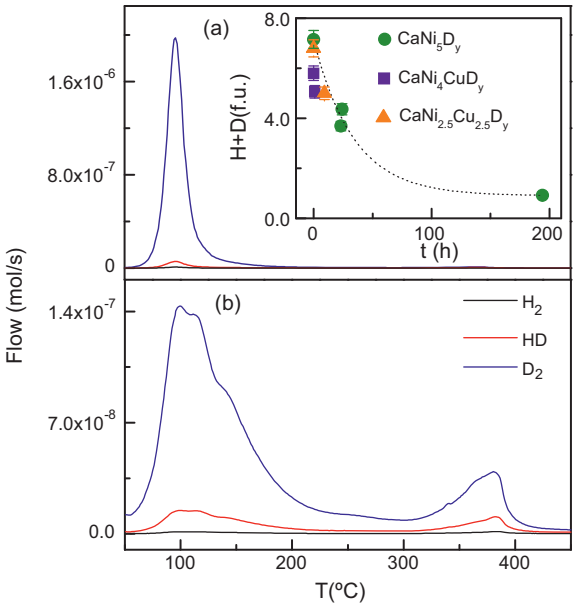

Fig. 3. Thermal desorption spectra for $CaNi_5D_y$. (a) Deuterium desorption after 24 h and (b) desorption after 194 h. Inset shows the evolution with time of the deuterium amount in the samples.

to the amorphous character of $CaNi_{2.5}Cu_{2.5}$, to the existence of inhomogeneties or to the similar stoichiometry of the sample to $CaNi_3$. it is worth highlighting the increment of desorption temperature as copper content increases, indicating the improved stability for the samples containing Cu atoms in the structure.

Inset of Fig. 3a represents the time evolution of the deuterium content in the samples after removing them from the Sieverts apparatus. The values of the quantity of deuterium absorbed by the samples during the first deuteration process are also included.

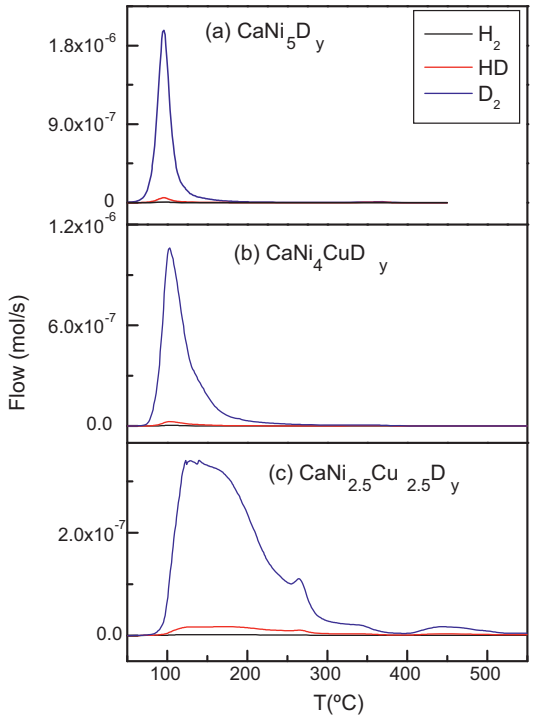

Fig. 4. Thermal desorption spectra of (a) $CaNi_5D_y$ (24 h after their deuteration), (b) $CaNi_4CuD_y$ (1 h after their deuteration) and (c) $CaNi_{2.5}Cu_{2.5}D_y$ (9 h after their deuteration).

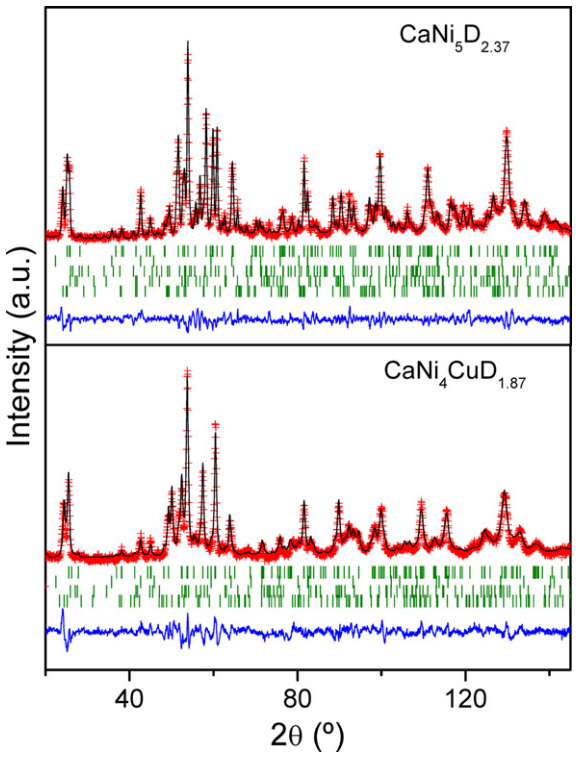

Fig. 5. Observed (crosses), calculated (full line) and difference (bottom) NPD Rietveld profiles for $CaNi_5D_y$ and $CaNi_4CuD_y$ at 295 K. The rest of the tick marks correspond to $Ca(OD)_2$, Ca_2Ni_7, $CaNi_3$ and $CaNi_3H_4$ impurities.

These compositions correspond to $CaNi_5H_{0.12}D_{4.24}$ (24 h after the deuteration), $CaNi_4CuH_{0.13}D_{4.93}$ (1 h after the deuteration) and $CaNi_{2.5}Cu_{2.5}H_{0.20}D_{4.80}$ (9 h after the deuteration). However, the spontaneous decomposition of the deuterides, due to their instability, lowers the amount of deuterium in the sample, as for instance down to 0.86 D/f.u. in the case of $CaNi_5D_y$ after 194 h from deuteration. Therefore, it is clear that the passivation of the samples after the deuteration is of paramount importance for applications.

3.3. Neutron powder diffraction studies

In order to study the crystallographic structure of the deuterides and to determine the amount of deuterium absorbed by the samples, neutron powder diffraction experiments have been performed. We have studied the crystallographic structures of $CaNi_5D_y$ and $CaNi_4CuD_y$ samples, whereas for $CaNi_{2.5}Cu_{2.5}D_y$ it was not possible to analyze the diffraction patterns since the sample was not crystalline enough.

The family of Ca–Ni deuterides presents a very complex phase diagram with four different phases depending on the quantity of deuterium on the compounds [16,22]. It has been identified a hexagonal α phase ($CaNi_5D_{0.3}$) in *P*6/*mmm* space group, two intermediate deuterium concentration orthorhombic phases α′ ($CaNi_5D_{0.9}$) and β ($CaNi_5D_{4.8}$), both in *Im*2*m*, and a final trigonal γ phase ($CaNi_5D_{6.1}$) in *P*31*m* with the highest deuterium concentration.

We have first refined the structure of the pure alloys before the deuteration, by using our NPD data. The intermetallic alloys $CaNi_5$ and $CaNi_4Cu$ are both defined in the hexagonal *P*6/*mmm* space group as it has been reported before [23]. In the case of the deuterated samples, both $CaNi_5D_y$ and $CaNi_4CuD_y$ structures have been refined using the orthorhombic space group *Im*2*m*, in which there are two different positions for Ca atoms (2*a* and 2*b*) and four

Table 1
Cell parameter, volume and reliability factors of $CaNi_{5-x}Cu_xD_y$ series at 295 K.

	$CaNi_5D_y$	$CaNi_4CuD_y$
*Im*2*m*		
a (Å)	8.6042(3)	8.656(2)
b (Å)	5.0984(2)	4.980(1)
c (Å)	7.8519(3)	7.949(2)
V (Å^3)	344.44(3)	342.66(2)
Occupancy		
Ni/Cu	1/0	3.8(3)/1.2(3)
D1 (8*e*)	0.11(3)	0.13(3)
D2 (4*c*)	0.21(2)	0.13(2)
D3 (4*c*)	0.82(4)	0.54(3)
D4 (4*d*)	0	0.14(3)
D5 (4*d*)	0	0.19(2)
D6 (8*e*)	0.43(2)	0.35(3)
D7 (8*e*)	0.23(3)	0.08(3)
Reliability factors		
χ^2	2.09	9.46
R_p	15.0	10.1
R_{wp}	15.3	14.1
R_I	10.58	4.58

positions for Ni atoms (4*c*, 4*c*, 4*d*, and 8*e*). The deuterium atoms can occupy seven different interstitial positions (8*e*, 4*c*, 4*c*, 4*d*, 4*d*, 8*e* and 8*e*). A NPD study had already been reported by Yoshikawa et al. [24], who found the distribution over seven different positions of the deuterium atoms in $CaNi_5D_y$. Our best refinement has been attained for the deuterium atoms occupying only the positions 8*e*, 4*c*, 4*c*, 8*e* and 8*e* in the case of $CaNi_5D_y$ and the seven positions in the case of $CaNi_4CuD_y$. Therefore, compared to Yoshikawa work we have found that in the case of $CaNi_5D_y$ the deuterium atoms are distributed over a reduced number of positions. The compositions obtained for both samples after the refinements are $CaNi_5D_{2.4}$ and $CaNi_4CuD_{1.9}$. The quantity of deuterium determined by NPD is smaller than the quantity determined by TDS. As we explained before, the samples are unstable and the quantity of deuterium

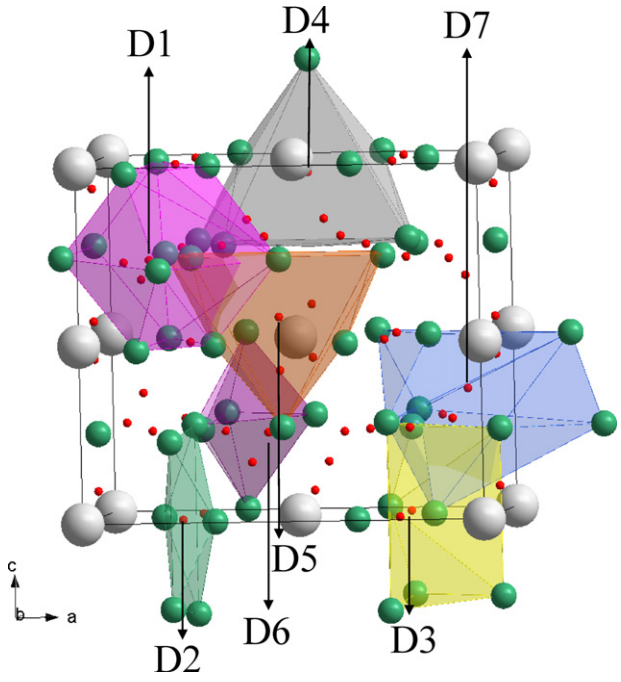

Fig. 6. Schematic view of the crystal structure of $CaNi_{5-x}Cu_xD_y$, with space group *Im*2*m*. Ca atoms are represented by the grey and biggest circles, Ni atoms by the middle-size green ones and D atoms by the red and smallest spheres. The Ni polyhedra around the deuterium atoms are drawn. (For interpretation of the references to color in this figure legend, the reader is referred to the web version of the article.)

diminishes with time. In the refinements it was necessary to introduce some impurities as secondary phases: $Ca(OD)_2$, Ca_2Ni_7, $CaNi_3$ and $CaNi_3H_4$. The good agreement between the observed and calculated data for both samples is illustrated in Fig. 5. Table 1 includes the final unit-cell parameters, volumes, occupancies and discrepancy factors after the refinements.

Fig. 6 shows a schematic view of the crystal structure of the deuterides. We have drawn the Ni polyhedron around the seven different deuterium sites (distances < 3.2 Å). Most of them are coordinated to six-nickel cations with similar polyhedral size. In the case of $CaNi_4CuD_y$ the deuterium atoms are randomly distributed over the seven different positions since in $CaNi_5D_y$ the deuterium only occupies five of these positions. The wider distribution found for the deuterium atoms all over the interstitials sites in the structure for $CaNi_4CuD_y$ can explain the higher stability of this sample versus $CaNi_5D_y$, since its deuterium desorption occurs at higher temperature. Moreover, this wider distribution can explain the slightly smaller volume of the Cu compound compared to $CaNi_5D_y$ (see Table 1), although Cu cations are larger than Ni cations. Therefore, this smaller volume is concomitant with the higher stability of the Cu compound.

4. Conclusions

We have prepared by arc-melting the intermetallic compounds $CaNi_5$, $CaNi_4Cu$ and $CaNi_{2.5}Cu_{2.5}$. The alloys have been deuterated in a Sieverts reactor, and they present an absorption capacity similar to the theoretical ones in only two absorption cycles. $CaNi_5$ achieves a deuterium concentration of 7.15 D/f.u., $CaNi_4Cu$ a concentration of 5.8 D/f.u. and $CaNi_{2.5}Cu_{2.5}$ absorbs 6.8 D/f.u. As it occurs in AB_5 alloys, in our samples the kinetics of the absorption process is extremely fast, even faster in the second absorption process than in the first one, due to the activation of the compounds. The absorption rate diminishes when the copper content increases. TDS spectra are similar for $x = 0$ and $x = 1$, while for $x = 2.5$ the spectra shows broader peaks due to inhomogeneties and low crystallinity of the sample. An increment of the desorption temperature occurs as Cu content increases, indicating the higher stability for the Cu samples. This result is in good agreement with NPD experiments, where we found that $CaNi_5D_y$ presents five different interstitial positions occupied by deuterium atoms, whereas in $CaNi_4CuD_y$ they occupy seven positions, which favours the higher stability of this compound.

Acknowledgements

We thank the financial support of the Spanish Ministry of Education and Science to the projects MAT2010-16404 and MAT2008-06547-C02-01, and we are grateful to ILL for making all facilities available.

References

[1] L. Schlapbach (Ed.), Hydrogen in Intermetallic Compounds, Springer, Berlin, 1988.
[2] J.A. Ritter, A.D. Ebner, J. Wang, R. Zidan, Mater. Today 9 (2003) 18.
[3] S. Seta, H. Uchida, J. Alloys Compd. 231 (1995) 448.
[4] H. Uchida, M. Sato, O. Moriwaki, J. Alloys Compd. 253/254 (1997) 235.
[5] P. Termsuksawad, S. Niyomsoan, B. Mishra, D.L. Olson, Z. Gavra, V.I. Kaydanov, Mater. Sci. Eng. B 117 (2005) 45.
[6] T. Takeshita, K.A. Gschneidner, J.F. Lakner, J. Less-Common Met. 78 (1981) 43.
[7] J. Chen, S.X. Dou, H.K. Liu, J. Power Sources 63 (1996) 267.
[8] J.G. Willems, Philips. J. Res. 39 (1984) 1.
[9] M. Jurczyk, W. Rajewski, W. Majchrzycki, G. Wójcik, J. Alloys Compd. 290 (1999) 262.
[10] B. Rozdzynska-Kielbik, W. Iwasieczko, H. Drulis, V.V. Pavlyuk, H. Bala, J. Alloys Compd. 298 (1/2s) (2000) 237.
[11] M. Latroche, A. Percheron-Guégan, Y. Chabre, J. Bouet, J. Pannetier, E. Ressouche, J. Alloys Compd. 231 (1995) 537.
[12] S. Luo, W. Luo, J.D. Clewley, Ted B. Flanagan, L.A. Wade, J. Alloys Compd. 231 (1995) 467.
[13] M. Geng, J. Han, D.O. Northwood, Int. J. Hydrogen Energy 22 (1997) 531.
[14] G.D. Sandrock, Proc. Int. Symp. on Hydrides for Energy Storage Geilo, August 1977, Pergamon, Oxford, 1978, p. 353.
[15] G.D. Sandrock, Proc. 12th Intersociety Energy Conversion Engineering Conf., vol.1, Washington, DC, American Nuclear Society, La Grange Park, IL, 1977, p. 951.
[16] G.D. Sandrock, J.J. Murray, M.L. Post, J.B. Taylor, Mater. Res. Bull. 17 (1982) 887.
[17] F. Leardini, J.F. Fernández, J. Bodega, C. Sánchez, J. Phys. Chem. Solids 69. (2008) 116.
[18] J.F. Fernandez, F. Cuevas, C. Sanchez, J. Alloys Compd. 298 (2000) 244.
[19] H.M. Rietveld, J. Appl. Crystallogr. 2 (1969) 65.
[20] J. Rodríguez-Carvajal, Physica B 192 (1993) 55.
[21] H. Oesterreicher, K. Ensslen, A. Kerlin, E. Buscher, Mater. Res. Bull. 15 (1980) 275.
[22] M.P. Pitt, H.W. Brinks, J.O. Jensen, B.C. Hauback, J. Alloys Compd. 372 (2004) 190.
[23] J.O. Jensen, N.J. Bjerrum, J. Alloys Compd. 185 (1999) 293–295.
[24] A. Yoshikawa, Y. Uyenishi, H. Iizumi, T. Matsumoto, N. Takano, F. Terasaki, J. Alloys Compd. 280 (1998) 204.